Heliyon 9 (2023) e18406

Contents lists available at ScienceDirect

Heliyon

journal homepage: www.cell.com/heliyon

Evaluation of physicochemical characteristics and centerline temperatures of Sr ceramic waste form

Byeonggwan Lee [a,b], Jung-Hoon Choi [a,*], Ki Rak Lee [a], Hyun Woo Kang [a], Hyeon Jin Eom [c], Kyuchul Shin [b,c], Hwan-Seo Park [a]

[a] Korea Atomic Energy Research Institute, 111 Daedeok-daero 989, Yuseong-gu, Daejeon, 34057, Republic of Korea
[b] Department of Hydrogen & Renewable Energy, Kyungpook National University, 80 Daehak-ro, Buk-gu, Daegu, 41566, Republic of Korea
[c] Department of Applied Chemistry, Kyungpook National University, 80 Daehak-ro, Buk-gu, Daegu, 41566, Republic of Korea

ARTICLE INFO

Keywords:
Waste burden minimization technology
Nuclide management process
Sr waste form fabrication
High-level waste
Ceramic waste form
$SrTiO_3$

ABSTRACT

When disposing of spent fuel, nuclides such as Cs-137 and Sr-90, which generate short-term decay heat, must be removed from the spent nuclear fuel for efficient storage facility utilization. The Korea Atomic Energy Research Institute (KAERI) has been developing a nuclide management process that can enhance disposal efficiency by sorting and collecting primary nuclides and a technology for separating Sr nuclides from the spent nuclear fuels using precipitation and distillation. In this study, we prepared Sr ceramic waste form, $SrTiO_3$, using the solid-state reaction method to immobilize the Sr nuclides, and its physicochemical properties were evaluated. Moreover, the radiological and thermal characteristics of the Sr waste form were evaluated by estimating the composition of Sr nuclides considering the spent nuclear fuel history such as burn-up and cooling period. The waste form was found to be stable with good mechanical strength and leaching properties in addition to a low coefficient of thermal expansion, which would be advantageous for intermediate storage. Based on the experimental and radiological results, the centerline temperature of the waste form caused by Sr-90 nuclide was estimated using the steady-state conduction equation. The centerline temperature increased with increasing diameter of the waste form. When generating the $SrTiO_3$ waste form using the Sr nuclide recovered after a cooling period of 10 years, the centerline temperature was estimated to exceed the melting point of $SrTiO_3$ at a diameter of 0.275 m, under all burn-up conditions. These results provide fundamental data for the management and intermediate storage of Sr waste.

1. Introduction

Strontium-90, which has a relatively short half-life of 28.8 years, releases 0.546 MeV energy through beta-emission and decay to yttrium-90. Y-90 decays to stable zirconium-90 with a half-life of 64.1 h and a high energy of 2.28 MeV through decay involving beta emission [1]. Owing to their properties such as pure beta radiation emission and high energy generation, strontium-90 and its daughter yttrium-90 are applied as beta particle sources, heat sources for radioisotope thermoelectric generators, and in targeted radiotherapy in nuclear medicine [2–6]. However, high-heat-generating nuclides such as Sr-90 and Cs-137 require a substantial disposal area owing to the restrictions on the heat generation of the disposal facility, thereby increasing the environmental burden [7]. Removing these

* Corresponding author.
E-mail address: mrchoijh@kaeri.re.kr (J.-H. Choi).

https://doi.org/10.1016/j.heliyon.2023.e18406
Received 15 March 2023; Received in revised form 17 July 2023; Accepted 17 July 2023
Available online 17 July 2023

high-heat-generating nuclides can aid in reducing the environmental burden of spent nuclear fuel disposal.

The Korea Atomic Energy Research Institute (KAERI) has been developing a technology to reduce the environmental burden by selectively separating primary fission nuclides such as high-heat-generating, long-lived, and high-mobility nuclides [8]. This technology primarily consists of nuclide management and waste form manufacturing processes. Based on their physicochemical properties, the nuclide management process includes the separation and capture of primary nuclides, such as Sr, CS, I, and TRU/RE.

Sr nuclides are dissolved in the chloride phase during the chlorination of U_3O_8 powder and are recovered in the form of carbonate or oxide via reactive distillation [8–10]. Subsequently, the Sr nuclides are fabricated as ceramic waste forms with high chemical durability while considering their intermediate storage and disposal. The Sr nuclide was fabricated in the form of $SrTiO_3$ with natural analogs. $SrTiO_3$ is one of ceramic waste form demonstrating high physicochemical stability, which is characterized by insolubility, high melting point (2080 °C), and high waste loading [1,11]. $SrTiO_3$ can be synthesized by various methods, including solid-state reaction, sol–gel, hydrothermal, and spark plasma [12,13], by which waste forms are fabricated for immobilizing radioactive Sr nuclides [13–16]. The waste forms that immobilize high-heat-generating nuclides generate significant heat per unit volume during intermediate storage periods; therefore, the waste forms require thermal management. In the Defense Waste Processing Facility at Savannah River Site, which manufactures glass waste forms to immobilize high-level radioactive waste, the high-level glass waste forms are stored in the Glass Waste Storage Building (GWSB) [17]. In the GWSB, a mechanical cooling system is operated to prevent overheating of the concrete vault and devitrification of the glass waste form in canisters because of decay heat [17,18]. Hence, estimating the centerline temperature is essential for evaluating the stability of the ceramic waste form containing high-heat-generating Sr nuclides and for controlling the cooling capacity of the intermediate storage facility.

Intermediate storage facilities for waste forms containing high-heat-generating nuclides are typically designed considering the total volume of the waste forms and heat generation of nuclides. In addition, these facilities are affected by the history of spent nuclear fuel such as burn-up or cooling (decay) period. The centerline temperature of the waste form is determined according to the waste loading of heat-generating nuclides and the diameter of the waste form. Therefore, from the perspective of the intermediate storage facility design, the amount of waste form and resulting centerline temperature must be evaluated considering each variable.

In this study, the $SrTiO_3$ waste form is fabricated via cold pressing/sintering based on the solid-state reaction. To calculate centerline temperatures, the physical and thermal properties of the Sr waste form are evaluated, and the radiological properties of the Sr ceramic waste form are estimated over 1000 years. Based on the experimental thermal properties and radiological evaluation, the centerline temperature of Sr waste form is calculated according to the diameter of the waste form and the history of spent nuclear fuel such as burn-up and cooling period considering the intermediate storage facility design.

2. Experimental

2.1. Materials

Deionized water obtained from a Milli-Q system purifier (Direct 16, Millipore Corp.) was used for all experiments. Strontium carbonate ($SrCO_3$, 99.9%) and titanium oxide (TiO_2, 99.5%, primary particle size = 21 nm) were purchased from Sigma–Aldrich. Ethanol (99.9%) was purchased from Daejung Chemicals. Polyvinyl alcohol (PVA, average M.W. = 1500) was purchased from Showa Chemical Industry. All reagents were used without further purification.

2.2. Waste form fabrication

In the nuclide management process, Sr nuclides are expected to be recovered in the form of oxides or carbonates. In this study, $SrCO_3$ and TiO_2 were selected as the starting materials, and the $SrTiO_3$ waste form was prepared using the cold pressing/sintering method based on the solid-state reaction: [$SrCO_3$ (s) + TiO_2 (s) → $SrTiO_3$ (s) + CO_2 (g)]. This method was selected because of the ease of manufacturing the bulk waste form, simplicity of fabrication, and straightforward application to the hot cell environment. The established waste fabrication process is shown in Fig. 1. The waste form fabricating process involves mixing of raw material powders, calcination, pelletizing, and sintering. The raw material powders, $SrCO_3$ (193.10 g) and TiO_2 (104.46 g), were measured to ensure a 1:1 M ratio of Sr to Ti. Ethanol (500 mL) was added to the raw material mixture, which was ground at 34,000 rpm for 5 min using a mechanical blender to obtain a homogeneous phase. The mixture was completely dried in an oven at 110 °C. After drying, the agglomerated mixture was pulverized into a fine powder using a mechanical blender. The powdered mixture was loaded on an alumina crucible, calcined for 5 h at 1200 °C using a high-temperature electric furnace under ambient atmosphere, and then slowly cooled.

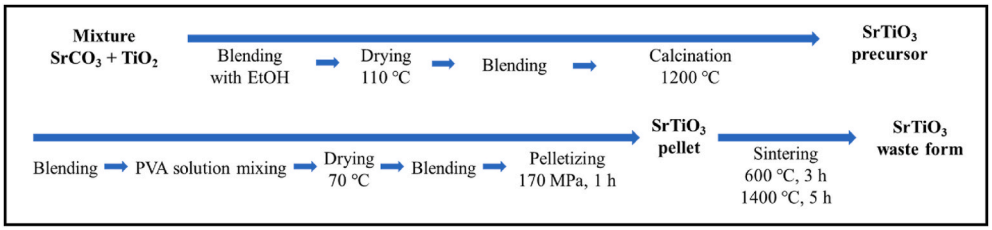

Fig. 1. Scheme of $SrTiO_3$ waste form fabrication.

After calcination, the $SrTiO_3$ precursor was pulverized into a fine powder using a mechanical blender. An aqueous solution of 6 wt% PVA was added to the precursor until the content of PVA reached 1 wt% relative to the mass of $SrTiO_3$ precursor. They were mixed to form a slurry, which was then completely dried in an oven at 70 °C. A punch/die with a diameter of 45 mm was used in the pelletizing process. The $SrTiO_3$ precursor powder (55 g) was loaded into the die and flattened and subsequently pressed at a uniaxial pressure of 170 MPa for 1 h to form a green body. The pellets were placed in a high-temperature electric furnace and maintained at 600 °C for 3 h for PVA de-binding, thereafter continuously heated to 1400 °C under a heating rate of 10 °C/min, sintered for 5 h, and slowly cooled to room temperature.

2.3. Evaluation of physicochemical properties

Crystal phase analysis was performed using powder X-ray diffraction (PXRD, SmartLab, Rigaku) to confirm the presence of by-products and unreacted substances in the produced $SrTiO_3$ waste form. Field-emission scanning electron microscopy (FE-SEM, SU5000, Hitachi) was utilized to investigate the morphology of the $SrTiO_3$ waste form cross-section in order to validate the microstructure. To evaluate the physical durability of the waste form, three-point bending strength measurements were performed using a universal testing machine (UTM, Instron 5848, Instron) for a specimen with dimensions of 3 mm × 4 mm × 36 mm. The chemical durability was measured using product consistency test method A (PCT-A) based on the procedure in ASTM C1285 [19]. The sintered $SrTiO_3$ waste form was crushed into powder using an agate mortar. According to the test procedure, the powders between 75 and 150 μm were obtained after pulverizing and sieving. Deionized water (20 g) was added to 2 g of the waste form, which was subsequently sealed and maintained at 90 °C for 7 days. After the PCT, the leachates were filtered using a 0.45 μm syringe filter, and the concentrations of Sr and Ti were measured using inductively coupled plasma-optical emission spectroscopy (ICP-OES, iCAP 6300 Duo, Thermo Fisher Scientific). The normalized release of the nuclide, r_i (g/m^2), was calculated through the following equation (1):

$$r_i = \frac{C_i}{f_i\left(\frac{A}{V}\right)} \tag{1}$$

where C_i (ppm) is the concentration of the nuclide, f_i is the mass fraction of the nuclide in the waste form, and A/V (1048 m^{-1}) is the ratio of the surface area to the volume. For evaluating the thermal properties, the thermal expansion coefficient was measured using a thermomechanical analyzer (TMA 402 F1, NETZSCH), specific heat using high-temperature differential scanning calorimetry (DSC 401 F1, NETZSCH), and thermal diffusivity using a laser flash apparatus (LFA 467, NETZSCH). The thermal conductivity (k) is calculated using equation (2):

$$''k = \rho \times \alpha \times C_p'' \tag{2}$$

where ρ is the density, α is the thermal diffusivity, and C_p is the specific heat. The apparent density of the waste form is used in this calculation.

2.4. Method of calculation

Using the Origen program [20], Radiological properties of Sr nuclides and Sr waste form were determined. The nuclide inventory was calculated using a Westinghouse CE 16 × 16 reactor type and 4.5 wt% uranium enrichment. The burn-up was changed at intervals of 15 GWd/MTU in the range of 30–75 GWd/MTU under a reactor power generation density of 37.5 MW/MTU. The decay was calculated using the inventory of Sr nuclides after 3 cycles of operation and cooling for 10, 20, and 30 years, respectively. To evaluate the radiological properties of the waste/waste form, the activity (Bq/g) and heat production (W/m^3) of Sr nuclides over a period of 1000 years were calculated using decay calculations. Using radiological properties and experimental thermal conductivity, the steady-state conduction equation for an infinitely long solid cylinder with thermal conductivity and uniform heat generation was utilized to calculate the centerline temperatures of the waste form relative to the burn-up and cooling periods [21].

3. Results

3.1. Physicochemical properties of $SrTiO_3$ waste form

The $SrTiO_3$ waste form manufactured through the established sintering process did not show any cracks. The green body and sintered $SrTiO_3$ waste form are shown in Fig. 2(a and b) and the FE-SEM images of the cross-section of the sintered $SrTiO_3$ waste form are shown in Fig. 3. The average apparent density of the sintered $SrTiO_3$ waste form was measured as 4.83 g/cm^2, which is 94.15% of the theoretical density (5.13 g/cm^2). Fig. 4 shows the PXRD pattern measured for crystal structure analysis. To determine the stability of the $SrTiO_3$ waste form during intermediate storage, the physicochemical and thermal properties were evaluated. To evaluate the mechanical strength of the sintered waste form, the three-point bending strength of the processed specimen was measured using a UTM; the results are displayed in Table 1. The average maximum flexural strength was confirmed to have a high bending strength of

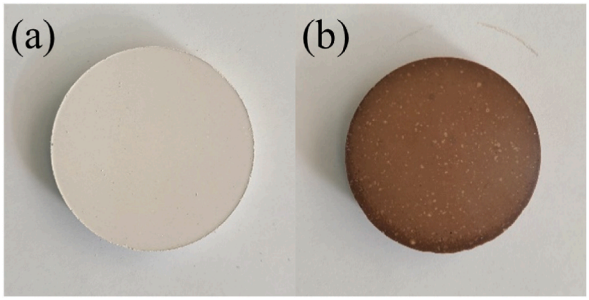

Fig. 2. $SrTiO_3$ pellets. (a) green body of the $SrTiO_3$ precursor; (b) sintered $SrTiO_3$ waste form. (For interpretation of the references to colour in this figure legend, the reader is referred to the Web version of this article.)

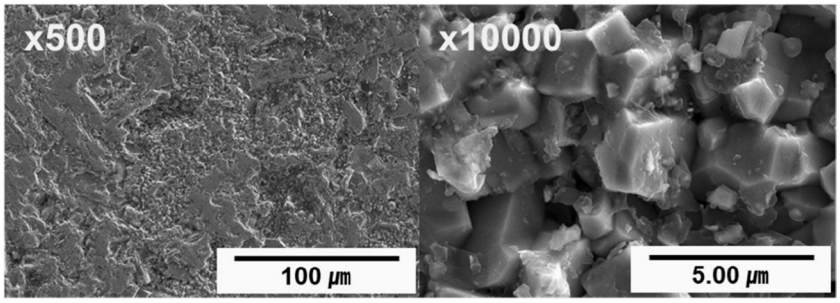

Fig. 3. FE-SEM image of a cross-section of $SrTiO_3$ waste form.

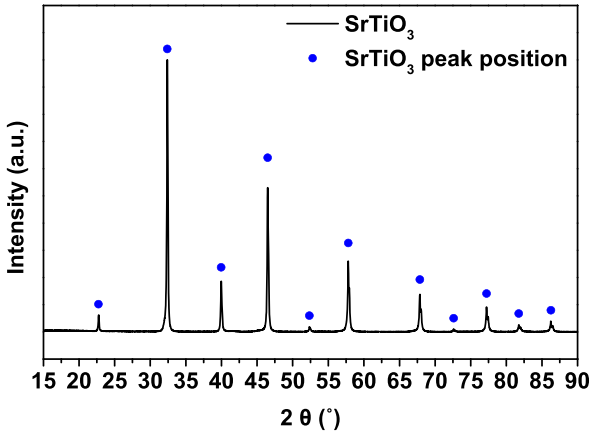

Fig. 4. Powder X-ray diffraction pattern of the $SrTiO_3$ waste form.

73.59 MPa. To evaluate the chemical durability, a leaching test of the waste form was performed using the PCT-A method. The leachate concentrations obtained through ICP-OES and the normalized leaching rate are listed in Table 2.

Fig. 5 shows the thermal expansion coefficients in the range of 15–985 °C that can be used to confirm the stability of $SrTiO_3$ owing to thermal expansion resulting from the heat generation. The coefficient of thermal expansion increases with increasing temperature, exhibiting the lowest value ($7.02 \times 10^{-6}\ K^{-1}$) at 15 °C and highest value ($1.27 \times 10^{-5}\ K^{-1}$) at 985 °C. Table 3 lists the specific heat and thermal diffusivity measured to evaluate the thermal properties of the $SrTiO_3$ waste form. The specific heat values are between 0.5 and 0.6 J/(g·K) in the measured temperature range (100–700 °C) and tend to converge after initially increasing with increasing temperature. The thermal diffusivity is 2.419 mm^2/s at 100 °C and decreases to 1.061 mm^2/s at 700 °C with increasing temperature. Fig. 6

Table 1
Three-point bending strength of the $SrTiO_3$ waste form.

Sample No.	Maximum flexural stress [MPa]
1	65.35
2	68.64
3	76.47
4	76.65
5	80.83
Average	73.59 (±5.70)

Table 2
Nuclide concentrations and normalized leaching rates of the leachate from product consistency test method A.

Sample No.	Sr concentration [ppm]	Ti concentration [ppm]	Normalized elemental mass release of Sr [g/m^2]
1	98.2	<0.01	0.196
2	147	<0.01	0.294
3	206	<0.01	0.412
4	166	<0.01	0.332
5	176	<0.01	0.352
6	74.1	<0.01	0.148
Average	145 (±45.4)	Under detection limit	0.289 (±0.09)

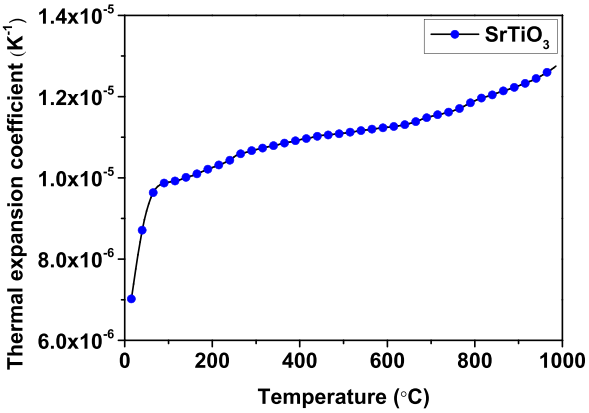

Fig. 5. Thermal expansion coefficient of the $SrTiO_3$ waste form.

Table 3
Thermal properties of the $SrTiO_3$ waste form.

Temperature [°C]	C_p [J/(g•K)]	Diffusivity [mm^2/s]
100	0.554	2.419
200	0.580	1.940
300	0.596	1.633
400	0.601	1.419
500	0.596	1.264
600	0.597	1.149
700	0.593	1.061

shows the calculated thermal conductivity (k), which is fitted with the equation "$k = aT^b$" to be expressed as a function of temperature [22,23]. The curve is well fitted (a = 693.74; b = −0.788; $R^2 = 0.9988$) to the calculated data. In section 3.2, the thermal conductivity was applied to the calculation of the centerline temperature of the Sr waste form.

3.2. Characterization of Sr waste/waste form

The compositions of Sr isotopes recovered from the nuclide management process were calculated according to the spent nuclear fuel history such as burn-up (30–75 GWd/MTU) and cooling period (10–30 years) and listed in Table 4. In addition, the total mass of Sr nuclides, the fraction of Sr-90, and the total mass, volume, and Sr waste loading of the Sr waste form generated under each burn-up and

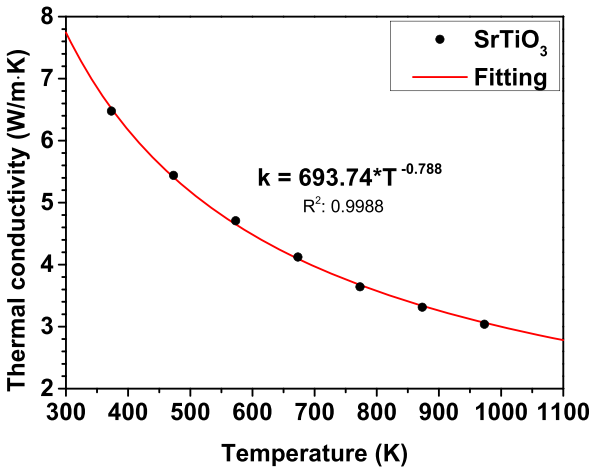

Fig. 6. Thermal conductivity of the $SrTiO_3$ waste form and the fitting curve.

Table 4
Mass and mass fractions of Sr nuclides generated from 1 MTHM of oxide spent fuel under each burn-up and cooling period.

Burn up [GWd/MTU]	Nuclides	Cooling Time [year]					
		10		20		30	
		Mass [g]	Mass fraction	Mass [g]	Mass fraction	Mass [g]	Mass fraction
30	Sr-84	6.415E−06	8.401E−09	6.415E−06	9.562E−09	6.415E−06	1.072E−08
	Sr-85	5.646E−25	7.394E−28	6.194E−42	9.233E−45	0.000E+00	0.000E+00
	Sr-86	2.800E−01	3.667E−04	2.800E−01	4.174E−04	2.800E−01	4.680E−04
	Sr-87	1.449E−03	1.898E−06	1.449E−03	2.160E−06	1.449E−03	2.422E−06
	Sr-88	3.383E+02	4.430E−01	3.383E+02	5.043E−01	3.383E+02	5.655E−01
	Sr-89	6.264E−21	8.203E−24	0.000E+00	0.000E+00	0.000E+00	0.000E+00
	Sr-90	4.250E+02	5.566E−01	3.323E+02	4.953E−01	2.597E+02	4.341E−01
	Total	7.636E+02	1.000E+00	6.709E+02	1.000E+00	5.983E+02	1.000E+00
45	Sr-84	1.492E−05	1.424E−08	1.492E−05	1.620E−08	1.492E−05	1.814E−08
	Sr-85	7.892E−25	7.534E−28	8.695E−42	9.438E−45	0.000E+00	0.000E+00
	Sr-86	6.502E−01	6.207E−04	6.502E−01	7.058E−04	6.502E−01	7.905E−04
	Sr-87	3.816E−03	3.643E−06	3.816E−03	4.142E−06	3.816E−03	4.639E−06
	Sr-88	4.686E+02	4.474E−01	4.686E+02	5.087E−01	4.686E+02	5.697E−01
	Sr-89	5.278E−21	5.039E−24	0.000E+00	0.000E+00	0.000E+00	0.000E+00
	Sr-90	5.782E+02	5.520E−01	4.520E+02	4.906E−01	3.533E+02	4.295E−01
	Total	1.047E+03	1.000E+00	9.213E+02	1.000E+00	8.226E+02	1.000E+00
60	Sr-84	2.731E−05	2.131E−08	2.731E−05	2.420E−08	2.731E−05	2.707E−08
	Sr-85	1.057E−24	8.246E−28	1.167E−41	1.034E−44	0.000E+00	0.000E+00
	Sr-86	1.191E+00	9.292E−04	1.191E+00	1.055E−03	1.191E+00	1.180E−03
	Sr-87	8.400E−03	6.553E−06	8.400E−03	7.442E−06	8.400E−03	8.325E−06
	Sr-88	5.792E+02	4.519E−01	5.792E+02	5.132E−01	5.792E+02	5.740E−01
	Sr-89	4.459E−21	3.479E−24	0.000E+00	0.000E+00	0.000E+00	0.000E+00
	Sr-90	7.014E+02	5.472E−01	5.483E+02	4.858E−01	4.286E+02	4.248E−01
	Total	1.282E+03	1.000E+00	1.129E+03	1.000E+00	1.009E+03	1.000E+00
75	Sr-84	4.361E−05	2.952E−08	4.361E−05	3.348E−08	4.361E−05	3.741E−08
	Sr-85	1.384E−24	9.368E−28	1.525E−41	1.171E−44	0.000E+00	0.000E+00
	Sr-86	1.905E+00	1.289E−03	1.905E+00	1.463E−03	1.905E+00	1.634E−03
	Sr-87	1.631E−02	1.104E−05	1.631E−02	1.252E−05	1.631E−02	1.399E−05
	Sr-88	6.745E+02	4.566E−01	6.745E+02	5.178E−01	6.745E+02	5.786E−01
	Sr-89	3.845E−21	2.603E−24	0.000E+00	0.000E+00	0.000E+00	0.000E+00
	Sr-90	8.009E+02	5.421E−01	6.261E+02	4.807E−01	4.894E+02	4.198E−01
	Total	1.477E+03	1.000E+00	1.303E+03	1.000E+00	1.166E+03	1.000E+00

Table 5
Total mass of Sr nuclides and fractions of Sr-90 in Sr nuclides, total mass and volume of the $SrTiO_3$ waste form fabricated under each burn-up and cooling period condition based on 1 MTHM of oxide spent fuel, and waste loading of the Sr waste form.

Burn-up [GWd/MTU]	Cooling period [year]	Sr nuclides		$SrTiO_3$		
		Mass [g]	Fraction of Sr-90 [wt%]	Mass [g]	Volume [m^3]	Waste loading of Sr [wt%]
30	10	763.6	55.66	1585.9	3.283E−04	48.15
	20	670.9	49.53	1394.4	2.887E−04	48.11
	30	598.3	43.41	1244.4	2.576E−04	48.08
45	10	1047.5	55.20	2175.6	4.504E−04	48.15
	20	921.3	49.06	1914.8	3.964E−04	48.11
	30	822.6	42.95	1710.9	3.542E−04	48.08
60	10	1281.8	54.72	2662.5	5.512E−04	48.14
	20	1128.7	48.58	2346.2	4.857E−04	48.11
	30	1009.0	42.48	2098.8	4.345E−04	48.07
75	10	1477.3	54.21	3068.8	6.354E−04	48.14
	20	1302.5	48.07	2707.6	5.606E−04	48.11
	30	1165.8	41.98	2425.2	5.021E−04	48.07

Table 6
Specific radioactivity of the Sr waste form fabricated under each burn-up and cooling condition.

Radioactivity [Bq/g $SrTiO_3$]										
Burn-up [GWd/MTU]	Cooling period [year]	Decay period [year]								
		0.1	0.3	1	3	10	30	100	300	1000
30	10	2.792E+12	2.778E+12	2.731E+12	2.600E+12	2.188E+12	1.337E+12	2.385E+11	1.732E+09	5.653E+01
	20	2.483E+12	2.471E+12	2.428E+12	2.312E+12	1.946E+12	1.189E+12	2.121E+11	1.540E+09	5.023E+01
	30	2.175E+12	2.164E+12	2.127E+12	2.025E+12	1.704E+12	1.041E+12	1.858E+11	1.349E+09	4.401E+01
45	10	2.769E+12	2.755E+12	2.708E+12	2.578E+12	2.170E+12	1.326E+12	2.365E+11	1.717E+09	5.604E+01
	20	2.459E+12	2.447E+12	2.405E+12	2.290E+12	1.927E+12	1.178E+12	2.101E+11	1.526E+09	4.980E+01
	30	2.151E+12	2.141E+12	2.104E+12	2.003E+12	1.686E+12	1.030E+12	1.838E+11	1.335E+09	4.354E+01
60	10	2.745E+12	2.731E+12	2.684E+12	2.555E+12	2.151E+12	1.314E+12	2.345E+11	1.702E+09	5.556E+01
	20	2.435E+12	2.423E+12	2.381E+12	2.267E+12	1.908E+12	1.166E+12	2.080E+11	1.511E+09	4.926E+01
	30	2.128E+12	2.117E+12	2.081E+12	1.981E+12	1.667E+12	1.019E+12	1.818E+11	1.320E+09	4.306E+01
75	10	2.719E+12	2.705E+12	2.659E+12	2.532E+12	2.131E+12	1.302E+12	2.323E+11	1.687E+09	5.502E+01
	20	2.409E+12	2.398E+12	2.356E+12	2.243E+12	1.888E+12	1.154E+12	2.058E+11	1.495E+09	4.878E+01
	30	2.103E+12	2.092E+12	2.056E+12	1.957E+12	1.647E+12	1.007E+12	1.796E+11	1.304E+09	4.256E+01

Table 7
Specific heat generation of the Sr waste form fabricated under each burn-up and cooling condition.

Heat generation [kW/m^3 $SrTiO_3$]										
Burn-up [GWd/MTU]	Cooling period [year]	Decay period [year]								
		0.1	0.3	1	3	10	30	100	300	1000
30	10	1.221E+03	1.215E+03	1.194E+03	1.137E+03	9.570E+02	5.849E+02	1.043E+02	7.574E−01	2.472E−08
	20	1.086E+03	1.081E+03	1.062E+03	1.011E+03	8.510E+02	5.201E+02	9.277E+01	6.737E−01	2.198E−08
	30	9.510E+02	9.463E+02	9.301E+02	8.855E+02	7.452E+02	4.554E+02	8.123E+01	5.899E−01	1.925E−08
45	10	1.211E+03	1.205E+03	1.184E+03	1.128E+03	9.490E+02	5.800E+02	1.035E+02	7.511E−01	2.451E−08
	20	1.075E+03	1.070E+03	1.052E+03	1.001E+03	8.428E+02	5.149E+02	9.188E+01	6.672E−01	2.177E−08
	30	9.409E+02	9.363E+02	9.203E+02	8.761E+02	7.373E+02	4.505E+02	8.037E+01	5.835E−01	1.904E−08
60	10	1.200E+03	1.195E+03	1.174E+03	1.118E+03	9.406E+02	5.748E+02	1.025E+02	7.446E−01	2.43E−08
	20	1.065E+03	1.060E+03	1.042E+03	9.915E+02	8.344E+02	5.100E+02	9.097E+01	6.606E−01	2.155E−08
	30	9.304E+02	9.260E+02	9.102E+02	8.663E+02	7.291E+02	4.456E+02	7.948E+01	5.772E−01	1.884E−08
75	10	1.189E+03	1.183E+03	1.163E+03	1.107E+03	9.319E+02	5.694E+02	1.016E+02	7.375E−01	2.407E−08
	20	1.054E+03	1.049E+03	1.030E+03	9.810E+02	8.258E+02	5.047E+02	9.001E+01	6.536E−01	2.133E−08
	30	9.194E+02	9.150E+02	8.995E+02	8.561E+02	7.207E+02	4.405E+02	7.855E+01	5.705E−01	1.861E−08

cooling period are presented in Table 5.

For Sr waste forms prepared from Sr nuclides that are recovered in each burn-up and cooling period, radiological properties such as radioactivity and heat generation resulting from the decay over 1000 years are presented in Tables 6 and 7, respectively. Fig. 7(a and b) and Fig. 8(a and b) show that the radiological properties of Sr waste forms according to the burn-up and cooling period for each representative case.

Subsequently, Using the scheme indicated in Fig. 9, the thermal conductivity and heat generation of the Sr waste form are used to compute the centerline temperature of the Sr waste form. Considering the cooling system in the intermediate storage facility, the

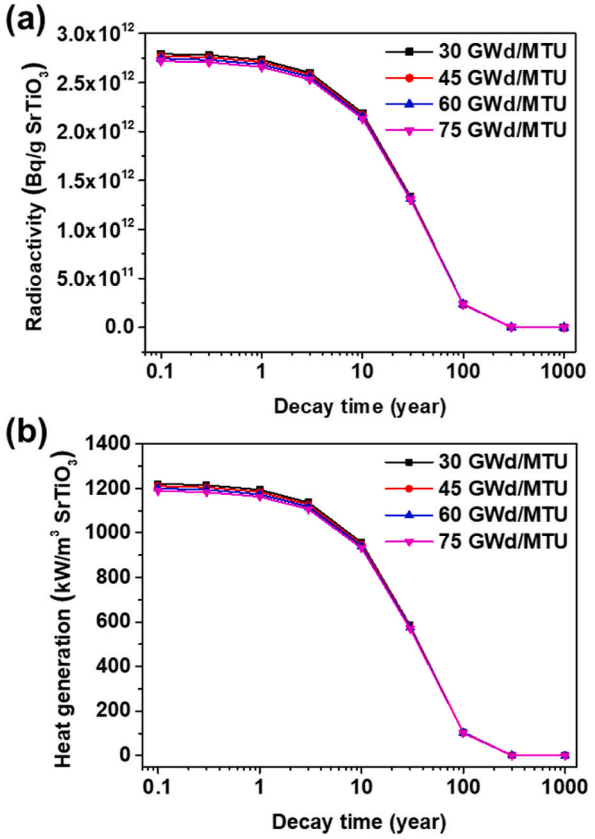

Fig. 7. Radiological properties of the Sr waste form fabricated after cooling for 10 years under each burn-up condition: (a) specific radioactivity and (b) specific heat generation.

surface temperature (T_s) of the waste form was set at 100 °C. The calculation is based on steady-state conduction (equation (3)) in a long, rigid, cylinder-shaped waste form with uniform heat generation. Moreover, simplification of the waste form geometry to a long infinite cylinder type consistently results in an overestimation of the centerline temperature compared to a finite height cylinder type waste form, as the infinite waste form is absent of top and bottom surfaces that can act as cooling surfaces. Hence, when assessing the thermal stability of the waste form, the simplification of the waste form geometry predicts higher centerline temperature therefore it is conservatively reasonable [21]. Equation (4), a one-dimensional heat conduction equation, is derived using equation (3) and boundary conditions. Equation (6), which indicates the temperature of the waste form in the radial direction r, is obtained by integrating equations (4) and (5); equation (5) is the fitted thermal conductivity as a function of temperature ($k = aT^b$) using the experimental data. Finally, equation (7) is used for calculating the central temperature.

$$\frac{1}{r}\frac{\partial}{\partial r}\left(kr\frac{\partial T}{\partial r}\right)+\frac{1}{r^2}\frac{\partial}{\partial \varphi}\left(\frac{\partial T}{\partial \varphi}\right)+\frac{\partial}{\partial z}\left(\frac{\partial T}{\partial z}\right)+\dot{q}=pc_p\frac{\partial T}{\partial t} \tag{3}$$

$$\frac{d}{dr}\left(r\frac{dT}{dr}\right)+\frac{\dot{q}}{k}r=0\ \left(B.C.:\left|\frac{dT}{dr}\right|_{r=0}=0\ and\ T(R)=T_s\right) \tag{4}$$

$$k=aT^b\ (a=693.74;\ b=-0.788) \tag{5}$$

$$T(r)=\left(T_s^{\,b+1}+\frac{\dot{q}(b+1)}{4a}\left(R^2-r^2\right)\right)^{\frac{1}{b+1}} \tag{6}$$

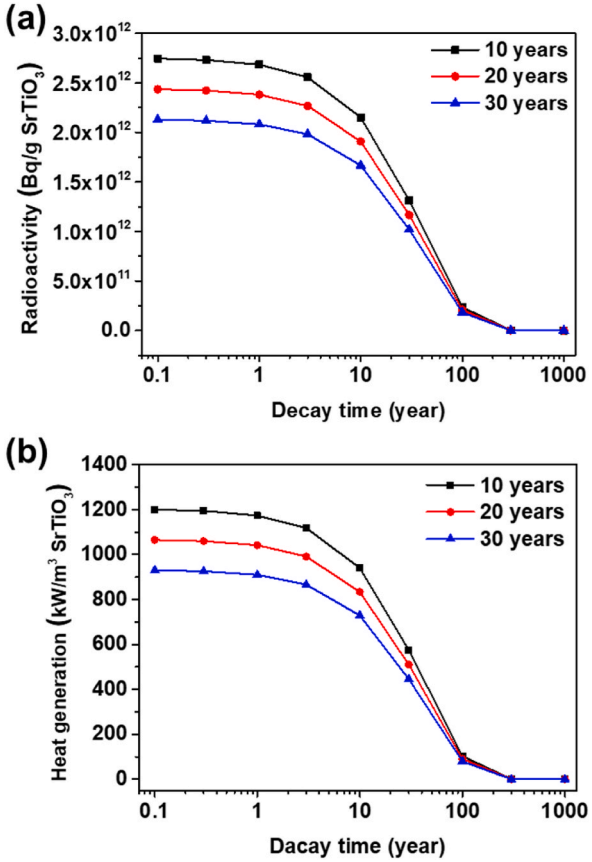

Fig. 8. Radiological properties of the Sr waste form fabricated after each cooling condition under 60 GWd/MTU: (a) specific radioactivity and (b) specific heat generation.

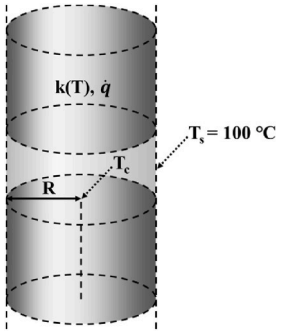

Fig. 9. Scheme of centerline temperature (T_c) calculation for the waste form with surface temperature (T_s), thermal conductivity (k), and heat generation (q).

$$T_{max} = T(r=0) = \left(T_s^{\,b+1} + \frac{\dot{q}(b+1)}{4a} R^2 \right)^{\frac{1}{b+1}} \tag{7}$$

Using equation (7), the centerline temperatures of the Sr waste form for various burn-up conditions, cooling periods, and diameters of the waste form are calculated according to the burn-up in Table 8, Table 9, Table 10, and Table 11, and displayed according to cooling periods in Fig. 10(a–d), Fig. 11(a–d), and Fig. 12(a–d).

Table 8
Centerline temperatures of the $SrTiO_3$ waste form for varying diameters and cooling periods of the spent nuclear fuel under the burn-up condition of 30 GWd/MTU.

Burn-up: 30 GWd/MTU		Centerline temperature of Sr waste form [°C]								
		Decay period [year]								
Cooling period [year]	Diameter [m]	0.1	0.3	1	3	10	30	100	300	1000
10	0.050	130.18	130.03	129.50	128.04	123.49	114.22	102.51	100.02	100.00
	0.075	170.58	170.21	168.93	165.40	154.49	132.60	105.66	100.04	100.00
	0.100	232.42	231.68	229.17	222.25	201.05	159.48	110.11	100.07	100.00
	0.125	321.70	320.39	315.94	303.71	266.68	196.08	115.89	100.11	100.00
	0.150	447.20	445.02	437.57	417.22	356.40	244.07	123.04	100.16	100.00
	0.175	621.48	617.95	605.95	573.31	477.16	305.69	131.63	100.22	100.00
	0.200	862.14	856.57	837.70	786.62	638.42	383.83	141.73	100.29	100.00
	0.225	1193.67	1185.06	1155.89	1077.33	852.96	482.20	153.40	100.37	100.00
	0.250	1649.87	1636.72	1592.23	1473.02	1137.85	605.50	166.76	100.45	100.00
	0.275	2277.04	2257.16	2190.06	2011.14	1515.81	759.68	181.90	100.55	100.00
20	0.050	126.74	126.61	126.14	124.86	120.84	112.63	102.23	100.02	100.00
	0.075	162.27	161.96	160.83	157.75	148.16	128.88	105.03	100.04	100.00
	0.100	216.14	215.53	213.33	207.35	188.90	152.55	108.98	100.06	100.00
	0.125	292.97	291.91	288.06	277.62	245.78	184.57	114.10	100.10	100.00
	0.150	399.45	397.70	391.36	374.24	322.63	226.25	120.44	100.15	100.00
	0.175	545.00	542.22	532.16	505.13	424.73	279.30	128.03	100.20	100.00
	0.200	742.63	738.32	722.77	681.18	559.16	345.93	136.93	100.26	100.00
	0.225	1010.16	1003.61	980.00	917.12	735.34	428.93	147.21	100.33	100.00
	0.250	1371.83	1361.99	1326.61	1232.83	965.70	531.83	158.93	100.40	100.00
	0.275	1860.33	1845.72	1793.28	1654.92	1266.58	659.01	172.19	100.49	100.00
30	0.050	123.34	123.23	122.82	121.70	118.20	111.04	101.95	100.01	100.00
	0.075	154.12	153.85	152.87	150.21	141.92	125.20	104.40	100.03	100.00
	0.100	200.35	199.81	197.94	192.82	177.02	145.71	107.85	100.06	100.00
	0.125	265.48	264.55	261.31	252.50	225.54	173.29	112.32	100.09	100.00
	0.150	354.45	352.94	347.68	333.45	290.35	208.93	117.85	100.13	100.00
	0.175	474.10	471.75	463.56	441.45	375.30	253.90	124.45	100.17	100.00
	0.200	633.77	630.19	617.75	584.31	485.53	309.82	132.19	100.23	100.00
	0.225	846.01	840.66	822.11	772.47	627.76	378.74	141.09	100.29	100.00
	0.250	1127.60	1119.73	1092.44	1019.75	810.76	463.21	151.23	100.35	100.00
	0.275	1500.87	1489.39	1449.69	1344.41	1045.85	566.37	162.66	100.43	100.00

Table 9
Centerline temperatures of the $SrTiO_3$ waste form for varying diameters and cooling periods of the spent nuclear fuel under the burn-up condition of 45 GWd/MTU.

Burn-up: 45 GWd/MTU		Centerline temperature of Sr waste form [°C]								
		Decay period [year]								
Cooling period [year]	Diameter [m]	0.1	0.3	1	3	10	30	100	300	1000
10	0.050	129.92	129.77	129.24	127.80	123.29	114.10	102.49	100.02	100.00
	0.075	169.94	169.58	168.31	164.83	154.01	132.32	105.61	100.04	100.00
	0.100	231.17	230.46	227.95	221.13	200.12	158.95	110.02	100.07	100.00
	0.125	319.47	318.22	313.78	301.73	265.09	195.20	115.75	100.11	100.00
	0.150	443.48	441.39	433.97	413.94	353.81	242.70	122.85	100.16	100.00
	0.175	615.47	612.09	600.16	568.08	473.12	303.66	131.36	100.22	100.00
	0.200	852.67	847.36	828.61	778.47	632.27	380.90	141.36	100.29	100.00
	0.225	1179.03	1170.81	1141.87	1064.85	843.77	478.05	152.94	100.36	100.00
	0.250	1627.51	1614.97	1570.89	1454.17	1124.30	599.73	166.17	100.45	100.00
	0.275	2243.25	2224.34	2157.93	1982.97	1496.05	751.75	181.17	100.54	100.00
20	0.050	126.48	126.35	125.89	124.61	120.63	112.50	102.21	100.02	100.00
	0.075	161.64	161.33	160.22	157.15	147.68	128.59	104.98	100.04	100.00
	0.100	214.92	214.31	212.15	206.20	187.97	152.00	108.89	100.06	100.00
	0.125	290.83	289.77	285.98	275.62	244.19	183.66	113.96	100.10	100.00
	0.150	395.93	394.19	387.95	370.98	320.08	224.85	120.24	100.14	100.00
	0.175	539.41	536.64	526.76	500.00	420.80	277.24	127.75	100.20	100.00
	0.200	733.97	729.69	714.44	673.31	553.27	343.00	136.56	100.26	100.00
	0.225	997.00	990.50	967.37	905.28	726.67	424.84	146.74	100.32	100.00
	0.250	1352.08	1342.34	1307.73	1215.25	953.13	526.20	158.34	100.40	100.00
	0.275	1831.02	1816.57	1765.34	1629.09	1248.54	651.36	171.45	100.48	100.00
30	0.050	123.09	122.97	122.57	121.47	118.00	110.92	101.93	100.01	100.00
	0.075	153.52	153.24	152.29	149.65	141.46	124.92	104.35	100.03	100.00
	0.100	199.19	198.65	196.81	191.76	176.14	145.19	107.77	100.06	100.00
	0.125	263.47	262.55	259.36	250.67	224.05	172.45	112.19	100.09	100.00
	0.150	351.19	349.69	344.53	330.50	287.98	207.64	117.65	100.13	100.00
	0.175	469.02	466.68	458.65	436.89	371.70	252.01	124.19	100.17	100.00
	0.200	626.05	622.49	610.31	577.44	480.22	307.15	131.83	100.22	100.00
	0.225	834.48	829.17	811.03	762.30	620.07	375.06	140.64	100.28	100.00
	0.250	1110.62	1102.82	1076.18	1004.92	799.79	458.21	150.66	100.35	100.00
	0.275	1476.14	1464.79	1426.09	1323.02	1030.36	559.66	161.95	100.42	100.00

Table 10
Centerline temperatures of the $SrTiO_3$ waste form for varying diameters and cooling periods of the spent nuclear fuel under the burn-up condition of 60 GWd/MTU.

Burn-up: 60 GWd/MTU		Centerline temperature of Sr waste form [°C]								
		Decay period [year]								
Cooling period [year]	Diameter [m]	0.1	0.3	1	3	10	30	100	300	1000
10	0.050	129.65	129.50	128.98	127.55	123.08	113.98	102.46	100.02	100.00
	0.075	169.29	168.93	167.67	164.21	153.50	132.02	105.56	100.04	100.00
	0.100	229.89	229.18	226.71	219.93	199.15	158.40	109.93	100.07	100.00
	0.125	317.20	315.96	311.58	299.62	263.40	194.27	115.61	100.11	100.00
	0.150	439.69	437.60	430.30	410.44	351.08	241.27	122.64	100.16	100.00
	0.175	609.36	606.00	594.26	562.48	468.85	301.53	131.07	100.22	100.00
	0.200	843.06	837.79	819.37	769.76	625.79	377.83	140.98	100.29	100.00
	0.225	1164.17	1156.02	1127.63	1051.54	834.09	473.72	152.44	100.36	100.00
	0.250	1604.84	1592.43	1549.25	1434.09	1110.06	593.72	165.55	100.45	100.00
	0.275	2209.06	2190.36	2125.39	1952.99	1475.32	743.50	180.40	100.54	100.00
20	0.050	126.22	126.08	125.63	124.36	120.42	112.38	102.19	100.02	100.00
	0.075	161.00	160.68	159.59	156.56	147.18	128.31	104.93	100.04	100.00
	0.100	213.67	213.04	210.93	205.06	187.02	151.48	108.80	100.06	100.00
	0.125	288.65	287.55	283.87	273.63	242.56	182.80	113.82	100.10	100.00
	0.150	392.34	390.53	384.47	367.73	317.47	223.52	120.03	100.14	100.00
	0.175	533.72	530.84	521.27	494.90	416.78	275.29	127.47	100.19	100.00
	0.200	725.18	720.74	705.98	665.50	547.25	340.21	136.19	100.25	100.00
	0.225	983.65	976.91	954.56	893.53	717.82	420.94	146.25	100.32	100.00
	0.250	1332.08	1321.99	1288.59	1197.83	940.31	520.85	157.73	100.40	100.00
	0.275	1801.37	1786.44	1737.07	1603.53	1230.15	644.11	170.70	100.48	100.00
30	0.050	122.83	122.72	122.32	121.22	117.80	110.80	101.91	100.01	100.00
	0.075	152.89	152.63	151.69	149.07	140.98	124.64	104.30	100.03	100.00
	0.100	197.98	197.47	195.66	190.64	175.23	144.68	107.68	100.06	100.00
	0.125	261.38	260.50	257.37	248.76	222.52	171.60	112.05	100.09	100.00
	0.150	347.80	346.38	341.32	327.42	285.55	206.35	117.46	100.12	100.00
	0.175	463.74	461.52	453.65	432.12	368.02	250.13	123.91	100.17	100.00
	0.200	618.02	614.67	602.74	570.26	474.78	304.50	131.47	100.22	100.00
	0.225	822.51	817.52	799.79	751.71	612.21	371.39	140.17	100.28	100.00
	0.250	1093.03	1085.70	1059.70	989.50	788.58	453.23	150.07	100.35	100.00
	0.275	1450.55	1439.90	1402.19	1300.79	1014.56	552.99	161.23	100.42	100.00

Table 11
Centerline temperatures of the $SrTiO_3$ waste form for varying diameters and cooling periods of the spent nuclear fuel under the burn-up condition of 75 GWd/MTU.

Burn-up: 75 GWd/MTU		Centerline temperature of Sr waste form [°C]								
		Decay period [year]								
Cooling period [year]	Diameter [m]	0.1	0.3	1	3	10	30	100	300	1000
10	0.050	129.36	129.22	128.70	127.29	122.87	113.84	102.44	100.02	100.00
	0.075	168.60	168.24	167.00	163.58	152.98	131.71	105.51	100.04	100.00
	0.100	228.53	227.82	225.38	218.70	198.15	157.82	109.84	100.07	100.00
	0.125	314.79	313.55	309.23	297.46	261.68	193.31	115.46	100.11	100.00
	0.150	435.66	433.58	426.40	406.87	348.28	239.78	122.42	100.16	100.00
	0.175	602.88	599.54	588.00	556.79	464.49	299.31	130.77	100.22	100.00
	0.200	832.88	827.64	809.57	760.91	619.17	374.63	140.58	100.28	100.00
	0.225	1148.45	1140.38	1112.55	1038.03	824.22	469.22	151.93	100.36	100.00
	0.250	1580.91	1568.62	1526.36	1413.73	1095.55	587.47	164.90	100.44	100.00
	0.275	2173.01	2154.52	2091.03	1922.64	1454.21	734.93	179.59	100.53	100.00
20	0.050	125.93	125.80	125.35	124.10	120.21	112.25	102.16	100.02	100.00
	0.075	160.32	160.01	158.92	155.93	146.67	128.00	104.88	100.04	100.00
	0.100	212.35	211.75	209.61	203.83	186.04	150.91	108.71	100.06	100.00
	0.125	286.34	285.28	281.56	271.51	240.89	181.86	113.67	100.10	100.00
	0.150	388.53	386.80	380.70	364.26	314.80	222.07	119.82	100.14	100.00
	0.175	527.69	524.95	515.31	489.46	412.67	273.15	127.17	100.19	100.00
	0.200	715.87	711.65	696.81	657.18	541.10	337.16	135.79	100.25	100.00
	0.225	969.53	963.15	940.70	881.05	708.79	416.70	145.74	100.32	100.00
	0.250	1310.96	1301.41	1267.93	1179.34	927.24	515.03	157.08	100.39	100.00
	0.275	1770.12	1756.01	1706.59	1576.45	1211.44	636.22	169.90	100.47	100.00
30	0.050	122.55	122.44	122.05	120.96	117.59	110.67	101.89	100.01	100.00
	0.075	152.24	151.97	151.04	148.46	140.49	124.35	104.25	100.03	100.00
	0.100	196.72	196.21	194.42	189.47	174.30	144.14	107.59	100.05	100.00
	0.125	259.20	258.33	255.26	246.76	220.95	170.72	111.91	100.09	100.00
	0.150	344.27	342.86	337.89	324.20	283.07	205.00	117.25	100.12	100.00
	0.175	458.25	456.05	448.34	427.16	364.25	248.16	123.63	100.17	100.00
	0.200	609.70	606.37	594.70	562.80	469.22	301.72	131.09	100.22	100.00
	0.225	810.12	805.17	787.86	740.70	604.18	367.57	139.68	100.28	100.00
	0.250	1074.85	1067.59	1042.25	973.50	777.15	448.04	149.45	100.34	100.00
	0.275	1424.15	1413.62	1376.91	1277.78	998.47	546.04	160.46	100.41	100.00

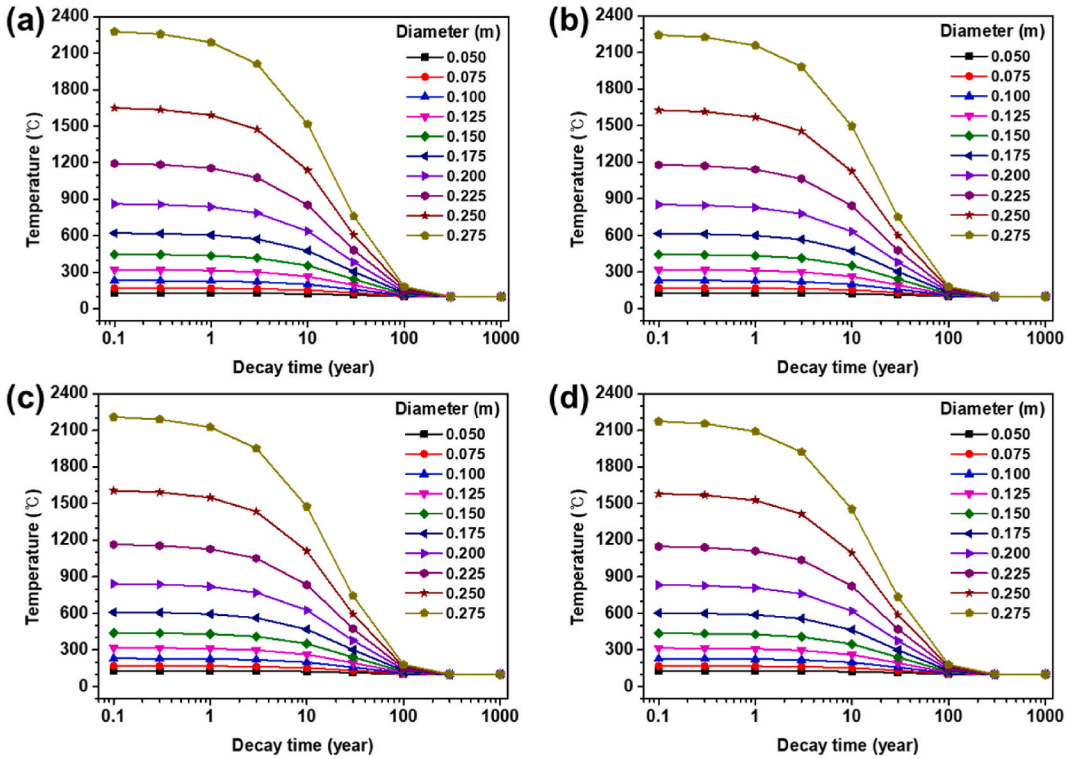

Fig. 10. Centerline temperatures for varying diameters of the Sr waste form and a cooling period of 10 years under the burn-up conditions of (a) 30, (b) 45, (C) 60, and (d) 75 GWd/MTU.

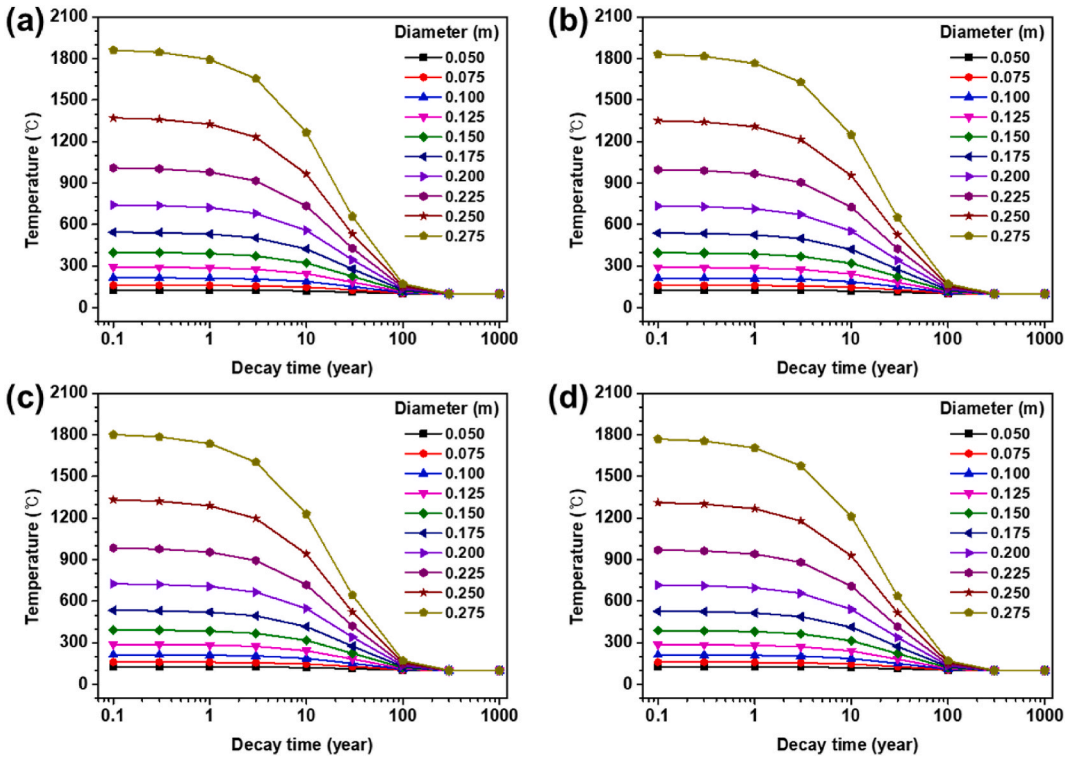

Fig. 11. Centerline temperatures for varying diameters of the Sr waste form and a cooling period of 20 years under the burn-up conditions of (a) 30, (b) 45, (C) 60, and (d) 75 GWd/MTU.

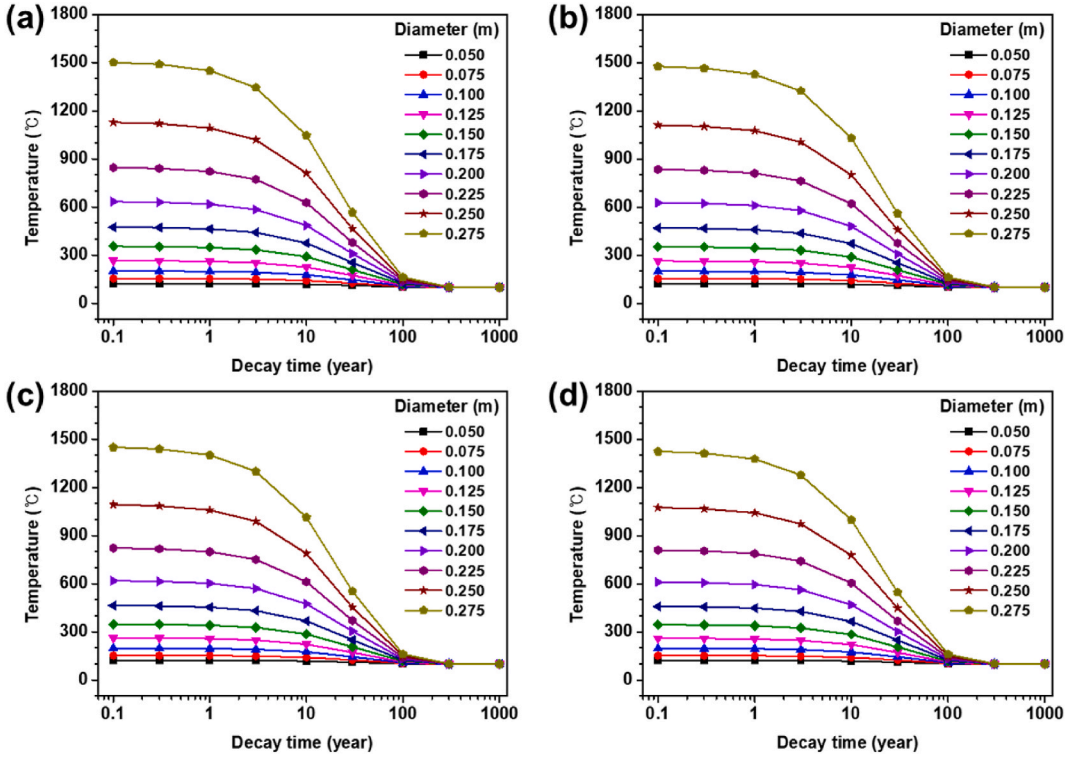

Fig. 12. Centerline temperatures for varying diameters of the Sr waste form and a cooling period of 30 years under the burn-up conditions of (a) 30, (b) 45, (C) 60, and (d) 75 GWd/MTU.

4. Discussion

4.1. Physicochemical properties of $SrTiO_3$ waste form

When the $SrTiO_3$ waste form was fabricated with the established process, a crack-free waste form was formed. The microstructure of the cross-section of the $SrTiO_3$ waste form was confirmed by FE-SEM images (see Fig. 3), which showed that the grains were well sintered and compact. It was also demonstrated that no porous structure was formed, resulting in a high apparent density (4.83 g/cm^2), which is 94.15% of the theoretical density. In addition, the peaks of the raw materials, $SrCO_3$ and TiO_2, were not observed through the PXRD analysis result, and only the $SrTiO_3$ peak existed (see Fig. 4). This result confirms that single-phase $SrTiO_3$ can be obtained using the established process without unreacted raw materials and side reactions. In PCT-A leaching test results (see Table 2), the concentration of Ti is a value below the detection limit. The low concentration of Ti in the leachate is attributed to the preferential leaching of monovalent and divalent cations from the surface of the waste form, resulting in an enrichment of the surface layer of insoluble TiO_2 [24]; these leaching characteristics were similarly evaluated for various titanate-based waste forms [25–28]. The normalized leaching rate of Sr nuclides is 0.298 g/m^2, and the leaching properties of the Sr nuclides are superior to those of environmental assessment glass [29]. Through physicochemical property evaluation, The $SrTiO_3$ waste form showed high bending strength in physical strength evaluation and low nuclide leaching rate in chemical durability evaluation.

The thermal expansion coefficient is sufficiently low (in the order of 10^{-6}–10^{-5}); thus, waste form expansion at high temperatures in the canister is not expected to present potential difficulties during intermediate storage or disposal. In addition, the measured thermal properties such as specific heat, thermal diffusivity, and thermal conductivity can be used as basic data for thermal management in intermediate storage and disposal of the Sr waste form. As a result of the evaluation of physicochemical and thermal properties, it was found that the waste form demonstrates excellent stability with good mechanical strength and leaching properties and low distortion of the waste form because of heat generation.

4.2. Characterization of Sr waste/waste form

According to Table 5, when the cooling period of spent nuclear fuel is constant, the total mass of Sr nuclides generated from 1 metric tons of heavy metal (MTHM) of oxide spent fuel increases on increasing the burn-up. Accordingly, the total mass of the $SrTiO_3$ waste form is considered to increase at high burn-up. Representatively, when comparing the amount of Sr nuclides for each burn-up after 10 years of cooling, the total mass of Sr nuclides increases to 763.6, 1047.5, 1281.8, and 1477.3 g as the burn-up is increased to 30, 45, 60, and 75 GWd/MTU, respectively. Hence, the total mass and volume of the $SrTiO_3$ waste form also increased. However, the

mass of the Sr nuclide normalized to the burn-up is found to be 25.45 g/GW at 30 GWd/MTU and 19.70 g/GW at 75 GWd/MTU; therefore, the higher the burn-up, the lower the fraction of Sr nuclide generated per unit energy generation. The fraction of Sr-90, which plays a dominant role in radioactivity and heat generation, slightly decreased with increasing burn-up; however, no significant difference was noted. The change in the Sr nuclide fraction at a constant cooling period owing to the difference in the burn-up condition also displays similar trends in the other cooling periods considered. For a constant burn-up condition, the change in the total mass of Sr nuclides with the cooling period is predominantly caused by the decay of the Sr-90 nuclides. As the cooling period is increased, the Sr-90 fraction decreases because of the decay of Sr-90, and thus the total mass of recovered Sr nuclides is decreased. Representatively, under the burn-up condition of 60 GWd/MTU, the total mass of Sr nuclides in nuclear fuel cooled for 10 years was 1281.8 g, and the fraction of Sr-90 was 54.72%. However, when the fuel is cooled for 30 years, the fraction of Sr-90 was 42.72%, and the total mass of Sr nuclides was 1009.0 g, which indicates a decrease of 22% relative to 10 years of cooling. In each burn-up condition, the Sr nuclide mass decreased at almost the same ratio as the cooling period increased, because each burn-up condition involves a similar fraction of Sr-90.

To compare the changes in the radiological properties owing to the burn-up, the specific radioactivity and specific heat generation of the Sr waste form fabricated from the recovered Sr nuclide after 10 years of cooling under each burn-up condition are shown in Fig. 7 (a and b). When the cooling period is constant, the radioactivity and heat generation of the Sr waste form are slightly decreased according to the increase of burn-up because the fraction of Sr-90 in the Sr nuclide decreases with increasing burn-up. However, a significant difference was not observed. The radiological characteristics of the Sr waste form fabricated after cooling for 10, 20, and 30 years following the burn-up condition of 60 GWd/MTU are compared, as shown in Fig. 8(a and b). As the cooling period was increased, the radioactivity and heat decreased at the same fraction; particularly, the radiological properties decreased by approximately 22% when the cooling period was increased from 10 to 30 years, thus indicating the same extent of decrease as that of the total mass of Sr-90. However, only a slight difference is observed in the reduction fraction owing to the change in the burn-up condition because the Sr-90 fraction is similar at the same cooling period.

For a constant diameter of the Sr waste form fabricated after cooling for 10 years (see Fig. 10), the centerline temperatures related to the varying burn-up conditions of the Sr waste form are predicted to be similar because of the similar specific heat generation. In contrast, the centerline temperature exponentially increases with increasing diameter. In particular, when the diameter of the waste form is 0.275 m, the centerline temperature of the waste form is predicted to increase to 2277 °C at 30 GWd/MTU and 2173 °C at 75 GWd/MTU. At this diameter, the centerline temperature exceeds the melting point (2080 °C) of $SrTiO_3$, which is detrimental to the stability of the waste form. Under the other conditions, the centerline temperature is not observed above the $SrTiO_3$ melting point. Moreover, after 300 years of decay, the centerline temperature of the waste form under all conditions is similar to the surface temperature. These estimated results of the centerline temperature of the Sr waste form can provide criteria for evaluating the stability of the waste form based on the spent nuclear fuel history and diameter of the waste form and can be used to control heat generation in Sr waste by adding non-heat generating Sr isotopes as dummy elements to satisfy the criteria of centerline temperature. Furthermore, they could be used to determine the arrangement the waste form canister, considering heat generation and heat conduction during canister loading, and utilized as a basis for adjusting the cooling capacity of intermediate storage and disposal facilities according to heat generation.

5. Conclusions

To reduce the environmental burden caused by the disposal of spent nuclear fuel, KAERI has been developing a nuclide management process for separating primary nuclides. In this study, $SrTiO_3$ waste forms were fabricated using cold pressing/sintering to immobilize high-heat-generating Sr nuclides recovered from the nuclide management process. Three-point bending strength and leaching performance (PCT-A) of the fabricated $SrTiO_3$ waste form were used to evaluate the mechanical and chemical durability, respectively. Additionally, thermal properties such as the coefficient of thermal expansion and thermal conductivity were determined. Through these physicochemical property evaluations, primary data on the material properties of the $SrTiO_3$ waste form were obtained. Furthermore, the radiological characteristics of Sr nuclides that could be recovered under various burn-up conditions and cooling periods of spent nuclear fuel were predicted. Based on the experimental and radiological results, the centerline temperatures of the $SrTiO_3$ waste form under various conditions such as diameter, burn-up, and cooling period were estimated. When the $SrTiO_3$ waste form was generated using the Sr nuclide recovered after 10 years of cooling under all calculated burn-up conditions, the centerline temperature exceeded the melting point of $SrTiO_3$ at a diameter of 0.275 m. These results concerning the estimation of the centerline temperature of the Sr waste form can provide criteria for evaluating the stability of a waste form according to the spent nuclear fuel history and diameter of the waste form. Furthermore, the findings can be used as preliminary data for managing waste forms with heat-generating nuclides in terms of the design of the canister, cooling capacity of the intermediate storage facility, and the disposal facility.

Author contribution statement

Byeonggwan Lee: Conceived and designed the experiments; Performed the experiments; Analyzed and interpreted the data; Wrote the paper.

Jung-Hoon Choi: Conceived and designed the experiments; Performed the experiments; Analyzed and interpreted the data.

Ki Rak Lee; Hyun Woo Kang; Hwan-Seo Park: Analyzed and interpreted the data; Contributed reagents, materials, analysis tools or data.

Hyeon Jin Eom; Kyuchul Shin: Analyzed and interpreted the data.

Data availability statement

Data included in article/supp. material/referenced in article.

Declaration of competing interest

The authors declare that they have no known competing financial interests or personal relationships that could have appeared to influence the work reported in this paper

Acknowledgments

This work was supported by the National Research Foundation of Korea (NRF) grant funded by the Korean government (MSIT) [NRF-2021M2E3A1040061 and NRF-2019M2D1A1059524].

References

[1] P. Pathak, D.K. Gupta, Strontium Contamination in the Environment, Springer International Publishing, Cham, 2020, https://doi.org/10.1007/978-3-030-15314-4.
[2] R. Shor, R.H. Lafferty Jr., P.S. Baker, Strontium-90 Heat Sources, Oak Ridge, TN (United States), 1971, https://doi.org/10.2172/4047957.
[3] K. Bikit, J. Knezevic, D. Mrdja, N. Todorovic, P. Kuzmanovic, S. Forkapic, J. Nikolov, I. Bikit, Application of 90Sr for industrial purposes and dose assessment, Radiat. Phys. Chem. 179 (2021), 109260, https://doi.org/10.1016/j.radphyschem.2020.109260.
[4] S. Laskar, L. Gurram, S.G. Laskar, S. Chaudhari, N. Khanna, R. Upreti, Superficial ocular malignancies treated with strontium-90 brachytherapy: long term outcomes, J. Contemp. Brachytherapy 5 (2015) 369–373, https://doi.org/10.5114/jcb.2014.55003.
[5] J.H. Harley, Fallout Strontium 90 as a metabolic tracer, Arch. Environ. Health 12 (1966) 578–582, https://doi.org/10.1080/00039896.1966.10664436.
[6] W.J.G. Oyen, L. Bodei, F. Giammarile, H.R. Maecke, J. Tennvall, M. Luster, B. Brans, Targeted therapy in nuclear medicine—current status and future prospects, Ann. Oncol. 18 (2007) 1782–1792, https://doi.org/10.1093/annonc/mdm111.
[7] G. Cerefice, L. Ma, Evaluation of Cs/Sr Waste Form for Long Term Storage and Disposal, 2008.
[8] J. Choi, B. Lee, K. Lee, H.W. Kang, H.J. Eom, S. Shin, G. Kim, H. Park, Characterization of waste generated from nuclide management process in waste burden minimization technology for spent nuclear fuel, Sci. Technol. Nucl. Install. 2022 (2022) 1–14, https://doi.org/10.1155/2022/4764825.
[9] H.C. Eun, J.H. Choi, N.Y. Kim, T.K. Lee, S.Y. Han, S.A. Jang, T.J. Kim, H.S. Park, D.H. Ahn, A study of separation and solidification of group II nuclides in waste salt delivered from the pyrochemical process of used nuclear fuel, J. Nucl. Mater. 491 (2017) 149–153, https://doi.org/10.1016/j.jnucmat.2017.04.060.
[10] S.-C. Jeon, J.-W. Lee, S.-J. Kang, J.-H. Lee, J.-W. Lee, G.-I. Park, I.-T. Kim, Temperature dependences of the reduction kinetics and densification behavior of U3O8 pellets in Ar atmosphere, Ceram. Int. 41 (2015) 657–662, https://doi.org/10.1016/j.ceramint.2014.08.118.
[11] O. Madelung, U. Rossler, M. Schulz, Ternary Compounds, Organic Semiconductors, Springer-Verlag, Berlin/Heidelberg, 2000, https://doi.org/10.1007/b72741.
[12] B.L. Phoon, C.W. Lai, J.C. Juan, P.L. Show, W.H. Chen, A review of synthesis and morphology of SrTiO3 for energy and other applications, Int. J. Energy Res. 43 (2019) 5151–5174, https://doi.org/10.1002/er.4505.
[13] E.K. Papynov, A.A. Belov, O.O. Shichalin, I.Y. Buravlev, S.A. Azon, E.A. Gridasova, Y.A. Parotkina, V.Y. Yagofarov, A.N. Drankov, A.V. Golub, I.G. Tananaev, Synthesis of Perovskite-like SrTiO3 ceramics for radioactive strontium immobilization by spark plasma sintering-reactive synthesis, Russ. J. Inorg. Chem. 66 (2021) 645–653, https://doi.org/10.1134/S0036023621050132.
[14] R. Zhang, Y. Gao, J. Wang, L. Li, W. Su, Leaching properties of immobilization of HLW into SrTiO3 ceramics, Adv. Mater. Res. 332–334 (2011) 1807–1811. https://doi.org/10.4028/www.scientific.net/AMR.332-334.1807.
[15] K. Zhang, G. Wen, D. Yin, H. Zhang, Preparation and aqueous durability of Sr incorporation into rutile TiO2, J. Wuhan Univ. Technol.-Materials Sci. Ed. 30 (2015) 1179–1183, https://doi.org/10.1007/s11595-015-1292-5.
[16] W. Mu, Q. Yu, X. Li, H. Wei, Y. Jian, Crystal structure stability of simulated Sr1–1.5xYxTiO3 (x = 0–0.12) waste forms, J. Wuhan Univ. Technol.-Materials Sci. Ed. 32 (2017) 89–93, https://doi.org/10.1007/s11595-017-1564-3.
[17] B.J. Hardy, Task Plan: Temperatures in DWPF Glass Waste Storage Building, Aiken, SC, 1993, https://doi.org/10.2172/10106557.
[18] R. Rainisch, Alternative Design Concept for the Second Glass Waste Storage Building, Aiken, SC, 1992, https://doi.org/10.2172/10105556.
[19] ASTM Standard C1285-21, Standard Test Methods for Determining Chemical Durability of Nuclear , Hazardous , and Mixed Waste Glasses and Multiphase Glass Ceramics : the Product Consistency Test (PCT), vol. 1, 2005, pp. 1–22, https://doi.org/10.1520/C1285-21.Copyright.
[20] O.W. Hermann, R.M. Westfall, ORIGEN-S: SCALE System Module to Calculate Fuel Depletion, Actinide Transmutation, Fission Product Buildup and Decay, and Association Source Terms, 1995.
[21] J.H. Choi, H.C. Eun, T.K. Lee, K.R. Lee, S.Y. Han, M.K. Jeon, H.S. Park, D.H. Ahn, Estimation of centerline temperature of the waste form for the rare earth waste generated from pyrochemical process, J. Nucl. Mater. 483 (2017) 82–89, https://doi.org/10.1016/j.jnucmat.2016.11.004.
[22] R. Wei, S. Song, K. Yang, Y. Cui, Y. Peng, X. Chen, X. Hu, X. Xu, Thermal conductivity of 4H-SiC single crystals, J. Appl. Phys. 113 (2013), https://doi.org/10.1063/1.4790134.
[23] Z. Gao, Z. Zhang, G. Liu, J.S. Wang, Ultra-low lattice thermal conductivity of monolayer penta-silicene and penta-germanene, Phys. Chem. Chem. Phys. 21 (2019) 26033–26040, https://doi.org/10.1039/c9cp05246a.
[24] A.E. Ringwood, V.M. Oversby, S.E. Kesson, W. Sinclair, N. Ware, W. Hibberson, A. Major, Immobilization of high-level nuclear reactor wastes in SYNROC: a current appraisal, Nucl. Chem. Waste Manag. 2 (1981) 287–305, https://doi.org/10.1016/0191-815X(81)90055-3.
[25] T. Murakami, T. Banba, H. Nakamura, Leaching of synroc-C: relation to microstructures, Nucl. Technol. 74 (1986) 299–306, https://doi.org/10.13182/NT86-A33832.
[26] T. Ringwood, Immobilization of Radioactive Wastes in SYNROC: a high-performance titanate ceramic waste form composed of minerals that have survived in various natural environments for long periods, SYNROC should permit safe burial of waste in deep drill holes, Am. Sci. 70 (1982) 201–207.
[27] T. Murakami, Crystalline product on surface of synroc after long leaching, J. Nucl. Mater. 135 (1985) 288–291, https://doi.org/10.1016/0022-3115(85)90093-5.
[28] D.M. Levins, R.S.C. Smart, Effects of acidification and complexation from radiolytic reactions on leach rates of SYNROC C and nuclear waste glass, Nature 309 (1984) 776–778, https://doi.org/10.1038/309776a0.
[29] C.M. Jantzen, N.E. Bibler, D.C. Beam, C.L. Crawford, M.A. Pickett, Haracterization of the Defense Waste Processing Facility (DWPF) Environmental Assessment (EA) Glass Standard Reference Material. Revision 1, Aiken, SC, in: C, 1993, https://doi.org/10.2172/10173249.